Single Mode Extraction from Multiple Modes of Lamb Wave

and Its Application to Defect Detection

Takahiro Hayashi[*]

and Koichiro Kawashima[*]

Key words: Ultrasonic Inspection, Nondestructive Inspection, Fast Fourier Transform, Lamb Wave, Signal Filtering, Air-Coupled Ultrasonic

*   Nagoya Institute of Technology, Gokiso-cho, Showa-ku, Nagoya-shi, Aichi, 466-8555

Japan

hayashi@megw.mech.nitech.ac.jp

Abstract

Lamb waves generally consist of many dispersive modes, which makes mode identification difficult. This study describes the extraction of a single mode from multiple modes. The single mode extraction is based on two-dimensional Fast Fourier Transform (2D FFT) in time and space, signal filtering, and 2D inverse FFT. An air-coupled ultrasonic technique was adopted for non-contact fast measurements. Using this technique, the A0 and S0 mode were clearly detected in preliminary tests of intact plates. Furthermore, multiple reflections of the A0 mode, which were shown only in the computer simulation, were experimentally confirmed in reflection tests of plates with a rectangular notch. In the reflection tests, two reflected waves were extracted in the intervals corresponding to notch widths.

1. Introduction

Lamb waves, propagating in a plate toward the longitudinal direction with flexural or dilatational vibrations, have great potential to long-range inspection for such large structures as pipelines and rails since they can propagate over long distances [1][2]. An oblique wedge or water has been normally used as a coupling medium to excite and receive Lamb waves. Recently wide varieties of applications have become promising due to the development of non-contact excitation and detection technique such as Laser ultrasonic[3] and air-coupled ultrasonic methods[4][5].

Lamb waves, however, propagate with very complex characteristics, varying with frequency, material properties, and thickness of a plate. And also many modes with different velocities can be excited at the same time. These characteristics make received signals difficult and prevent Lamb waves from being applied into non-destructive evaluation for plates. Figures 1 (a) and (b) show dispersion curves for phase velocity and group velocity, respectively. The horizontal axis is the product of frequency f and plate thickness d, and the vertical axis is phase velocity c and group velocity c_g, respectively. Larger slope of the curves means higher dispersion, and many curves at a fd value means that many propagating modes exist at the fd value. Waves are largely distorted with propagating distance in the high dispersive region, and many modes of Lamb wave are detected in the region with many curves. In many mode regions, Lamb wave analysis from RF signals is very difficult since many modes with different velocities are shown in the RF signals. In the practical non-destructive evaluation (NDE), only non-dispersive S0 mode shown in a gray region of Fig.1 is applied to NDE of a plate due to its prominent characteristic of single mode excitation and detection.

An A0 mode has a weak dispersive characteristic in the broad fd range as shown in Fig.1. The A0 mode with the velocities below Rayleigh wave velocity c_R cannot be efficiently excited and received with a wedge transducer or water immerged technique. Figure 2 shows dispersion curves with the representation of critical angles ($\theta=\sin^{-1}(c_w/c)$) for an oblique incidence and detection techniques using a polymer wedge (sound speed c_w=2520m/s) and air (sound speed c_w=340m/s). Since the critical angle of A0 mode are very large over 60 degrees in the polymer

wedge, an ultrasonic transducer cannot be adjusted to the critical angle in practice. So, when the transducer angle is apart from the critical angle, a single A0 mode cannot be excited and received, and unwanted S0 and higher modes can be superimposed in RF signals. Especially in such materials with low ultrasonic velocities as plastic plates, an A0 mode is not easily handled due to its low velocities and the resulting critical angle problem. Thus the authors presented that the critical angles for the A0 mode become suitable values with air coupled transducers [5], in which incident wave is excited in the frequency region around the cut off frequency of A1 mode. Though the critical angle problems described above can be solved by the use of air-coupled transducers, unwanted higher modes are superimposed in the higher frequency region due to their close phase velocities.

In this study, therefore, a filtering technique where a single mode of Lamb wave is extracted from RF signals with multi-modes is developed. Moreover, multiple A0 mode reflections from edges of a notch are extracted from noisy waves including a lot of modes. The extracted A0 mode signals enable us to measure the width of a notch from the time difference of the multiple pulse echoes.

2. Key concept of single mode extraction

Figure 3 shows a key concept of single mode extraction. First of all, RF signals of Lamb wave are recorded in the time domain at many discrete positions in the Lamb wave propagation direction (Fig.3 (a)). Applying two-dimensional fast Fourier transform to two-dimensional recorded data set in the time and space directions, a two-dimensional FFT image with respect to wave number k and frequency f (k-f map) are obtained (Fig.3(b)). Next, a filtering function $F(k, f)$ that retains a mode of interest and eliminates unwanted modes is applied to the k-f map, where the filtering function $F(k, f)$ is determined by the theoretical dispersion curves (Fig.3 (c)). Applying two-dimensional inverse FFT to the filtered k-f map gives extracted waveforms for a single Lamb mode (Fig.3 (d)).

3. Experiment

A0 mode and S0 mode extractions are carried out for an aluminum plate of 5mm thickness. An oblique wedge transducer is used to transfer sufficient energy to plates. An air-coupled transducer is adopted as a non-contact receiver for fast scanning measurement. The angle beam wedge transducer, consisting of Panametrics V402SB and a polyimido block (c_w=2520m/s) designed to be the incident angle of 60°, adhere to the surface of a plate with the weight of 500gf and gel type coupling medium. An air-coupled receiver, Micro Acoustic Ltd. Model BAT^{TM}-1, moves precisely with a linear stage controlled by a PC with the Labview. The incident transducer V402SB is a broadband transducer with a center frequency of about 2.0MHz. Received signals, however were shift to 0.5MHz center frequency due to the high attenuation at the high frequency in air. The incident and receiving angles were adjusted to 60° and 8°, respectively, so as to be critical angles for the A0 mode at fd=0.5MHz x 5.0mm. Ritec SP-801 and BR-640 were used as a pulser and a receiver, and detected signals were recorded by a digital oscilloscope with 10MHz sampling frequency and 256 averaging. 100 waveforms were recorded at different points with 1.0mm increments in the propagation direction of Lamb wave. Since the Labview operated scanning and recording automatically, it took about one second to measure a waveform at one point. In practice, data acquisition system for 100-point measurements will reduce the data acquisition time and will enable in situ imaging of k-f map.

Filtering function $F(k,f)$ was a Hanning window function as,

$$F(k,f) = \begin{cases} 0.5 + 0.5\cos\left\{\dfrac{2\pi(k-k_X)}{w}\right\}, & |k-k_X| < \dfrac{w}{2} \\ 0, & |k-k_X| > \dfrac{w}{2} \end{cases} \qquad (1)$$

The center of this Hanning function k_X, the wavenumber of mode X (X=A0, S0, ….), is theoretically obtained as a function of frequency f. The window width w is 50, 200, 350 [m^{-1}]. This function works to retain a desired mode X and to eliminate the other unwanted modes.

4. Results and discussions

4.1 Extraction of a single mode in an intact plate

A single A0 or S0 mode in an intact aluminum plate (A1100PM24, 500x100x5m) is extracted as preliminary tests. Figure 4 shows the experimental set-up. The distance of Lamb wave propagation is 231mm at the first receiver point (No.1) and 330mm at the last point (No.100).

Received waveforms at the three representative locations of the 25th, 50th, and 75th points are shown in Fig.5. The A0 mode had large amplitude because the incident and receiving angles were decided to be critical angles for A0 mode. Frequency f x thickness d region (fd region) used in this study is from about 1 to 4 MHz mm, which is shown in the group velocity dispersion curves of Fig.5. The group velocity dispersion curves in Fig.5 show that an A0 mode is non-dispersive and an S0 mode has very strong dispersion. And also group velocity of S0 mode wave is lower than that of A0 mode wave in the fd region from 2 to 3 MHz mm.

Figure 6 shows k-f distribution image obtained by the two-dimensional FFT of 100 waveforms, as well as theoretical dispersion curves. The k-f map shows two modes with high intensity; one is an A0 mode wave with very high intensity in the broad frequency region and the other one S0 mode wave around the region where an S0 and an A0 mode have close wavenumbers.

k-f maps after filtering for A0 mode and S0 mode extraction using filtering function of Eq. (1) are shown in Figs.7(a) and (b), respectively, where the width of window w is 200 m^{-1}. Extracted A0 mode waves (black) and S0 mode waves (gray) were obtained by inverse FFT of the filtered k-f maps as shown in Fig.8. A0 and S0 modes were separately obtained as expected, but wave packets were clearly seen in the different time from the raw signals in the filtered waveforms at the points close to the starting point No.1 or ending point No.100. For example, unwanted wave packets before the arrival time of A0 mode are seen in the waveforms at No.25 and No.75 (Fig.8, dotted circle). This is a FFT leakage error that happens because the first and the last waveforms are periodically connected in FFT and inverse FFT in the space direction.

4.2 Reduction of leakage error

In order to remove the leakage error in the extracted waveforms, Hanning window function, working for the first and last data sequences to be zero, is applied. Figure 9 shows the waveforms after extracting A0 mode and reducing the leakage error. Similarly to Figs.5 and 8, only waveforms at the typical three locations, No.25, No.50, and No.75, are shown in Fig.9. The leakage errors in the waveform at No.50 in Fig.9 were largely reduced compared to those in Fig.8. In No.25 and No.75, data sequences close to the edge, however, the errors could not be perfectly eliminated. Thus analysis of waveforms should be done with the filtered waveforms at No.50, the center of the date sequences in the space direction.

Measurement points should be less from the practical point of view. But less data in the space direction cause the leakage error of FFT and less resolution due to the lack of efficient data. Figure 10 shows extracted waveforms of A0 mode obtained with different observation points from 20 to 100. All waveforms shown in Fig.10 are representative one at the center of observation points out of many filtered waveforms from 20 to 100, having the least leakage errors due to the above mentioned reason. Less observation points caused the reduction of amplitude of waveforms. The FFT leakage errors were shown in the observation number of 60 or less. In the case of 20 observation points, the waveform of A0 mode is not clear and shows the reduction of filtering resolution as well as the leakage errors. Thus all results shown below are obtained with 100 observation points and with Hanning window in the space direction.

4.3 Effect of extracted waveforms by filtering functions

Extracted waveforms are strongly affected by the filtering functions. In this section, extracted waveforms of A0 mode are compared with different window width of w=50, 200, and 350 in Hanning function. Figure 11 shows extracted waveforms at No.50. And also Fig.12 shows k-f image after filtering by different Hanning functions with w=50, 200, and 350. When the window width is too narrow, w=50, the extracted waveform became small and the leakage errors could not be eliminated. When the width is broad, w=300, small S0 mode still remains in the extracted waveform.

Thus the window width *w*=200 is used in all results shown below.

4.4 Extraction of reflected waves from a notch

Lamb wave modes can be identified for intact plates even without using the above-mentioned filtering technique. Lamb waves in a plate with defects, however, are very complex due to mode conversions and multiple reflections at the defects. In this section, the propagation paths at a notch in plates are revealed by the use of filtering technique for A0 mode extraction.

The authors presented the multiple reflections at a delamination in layered plates with numerical analysis [6]. Similar multiple reflections can be seen at a notch in a plate. Figure 13 shows calculation results where Lamb waves are excited in a plate with a notch of 30mm width in the same configuration as the experiments. An A0 mode of Lamb wave propagates toward the notch in Fig.13(a), and then it separates into reflected and transmitted waves at the left edge of the notch (Fig.13 (b)). The transmitted wave, after propagating toward the right edge, separates again into transmitted and reflected waves at the right edge of the notch (Fig.13 (c)). This repetition results in the multiple reflections at a notch. The reflected waves at the edges of a notch, however, consist of S0 mode and the other higher modes as well as A0 mode. Therefore the multiple reflections cannot be observed in received signals.

Thus A0 mode is extracted from reflected Lamb waves in a plate with a notch to identify the reflected waves from both edges of a notch. Reflected waves were measured in the configuration shown in Fig.14. Raw signals (black) and filtered signals (gray) are shown in Fig.15, for the different notch width of L=10mm, 20mm, and 30mm, at No.25, No.50, and No.75, in which all filtered signals are doubled. Figure 16 shows the *k-f* map before filtering. Different from the *k-f* map for an intact plate as shown in Fig.6, many kinds of modes such as S0, A1 are included. Received raw signals (Fig.15 black) do not show the multiple reflections due to the wave packets marked by dotted circles. On the other hands, wave packets in the circles are eliminated in filtered waveforms shown by gray lines in Fig.15, and so the first reflected wave from the left edge (large arrow) and the

second reflection from the right (small arrow) can be clearly seen. The time interval between the first and the second reflected waves is proportional to the width of the notches, which implys that the filtered waveforms give information of the width of the notches. The time intervals between the two waves calculated by the cross correlation method are shown in Fig.17, as well as a theoretical line for the group velocity of 3142m/s, a value obtained from theoretical dispersion curves at fd=center frequency 0.5MHz x thickness of the notch 2.5mm. The measured values agree well with the theoretical line and it can be concluded that the measurements of Lamb wave at many points and the extraction of A0 mode give the approximated width of the notch in plates.

5 Conclusions

A single mode extraction technique was developed to improve analysis of Lamb wave in which multi-modes often superimposes. In this technique, the non-contact air coupled transducers enabled to perform easy and fast measurements of Lamb wave at many positions. This extraction technique was validated in the tests for intact aluminum plates and for plates with a rectangular notch. For plates without any notches, A0 and S0 modes were clearly separated. In the tests for plates with a rectangular notch, reflected waves from the both edges of the notch were recognized, and the approximate width of the notch was measured.

References

(1)   Vikrtov I. A., Rayleigh and Lamb Waves, (1967) Plenum

(2)   Rose J. L., Ultrasonic waves in solid media, (1999) Cambridge Press

(3)   Scruby C. B. and Drain L. E., Laser Ultrasonics Techniques and Applications, (1990) Adam Hilger

(4)   Shindel D. W. and Huchins D. A., Ultrasonics **33**-1 (1995), 11

(5)   Hayashi T. et. al., J. of JSNDI,(in Japanese), **50**-2 (2001), 108

(6)   Hayashi T. and Kawashima K., Ultrasonics, **40** (2002), 193

(7)   Hayashi T. et. al., Trans. Jpn. Soc. Mech. Eng., (in Japanese), **65**-630 (1999), 210

(8)   Hayashi T. and Endoh S., Ultrasonics, **38** (2000), 770

(9)   Eigenhardt C., Jacobs J. and Qu J., Review of progress in Quantitative Nondestructive Evaluation (2000)

Fig.1 Dispersion curves for an aluminum plate. (c_L=6300m/s, c_T=3100m/s)

Fig.2 Dispersion curves described by critical angles.

Fig.3 Key concept of single mode extraction.

Fig.4 Experimental set-up.

Fig.5 Waveforms in intact plate tests.

Fig.6 *k-f* distribution image for intact-plate tests.

Fig.7 *k-f* image after filtering.

Fig.8 Filtered waveforms in A0 and S0 extraction tests.

Fig.9 Waveforms when Hunning window is applied to the sequences in the space direction.

Fig.10 Comparison of waveforms for different number of obsevation points.

Fig11 Comparison of waveforms for different widow widths.

Fig.12 *k-f* image after filtering by different window widths.

Fig.13 Calculation results of A0 mode propagation around a square notch.

Fig.14 Experimantal set-up in reflection tests.

Fig.15 Sampled and filtered signals for different notch widths and different observation points.

(Large arrow indicates the reflected wave from the left edge of notch, and small arrow from the right

edge.)

Fig.16 *k-f* image for reflection tests.

Fig.17 Intervals of reflected waves for different notch widths.

Figure 1   Takahiro Hayashi
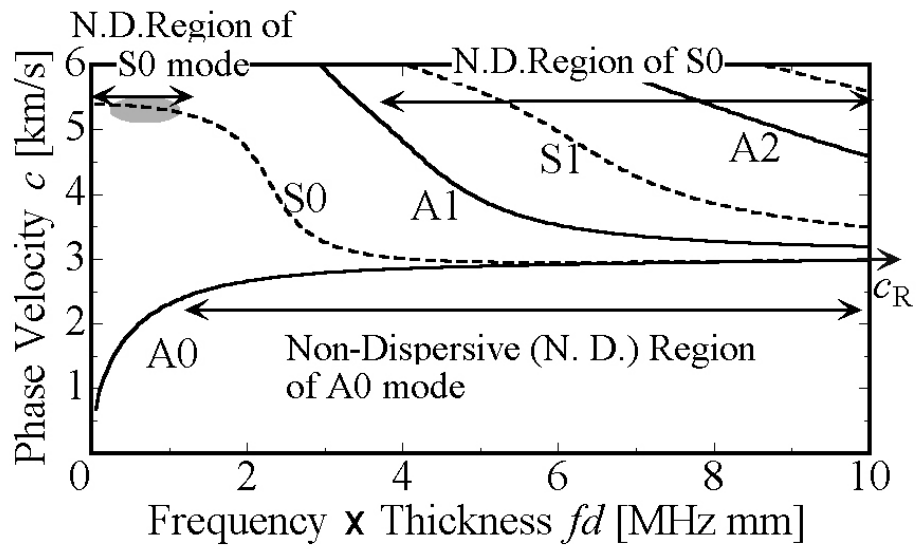
(a) phase velocity
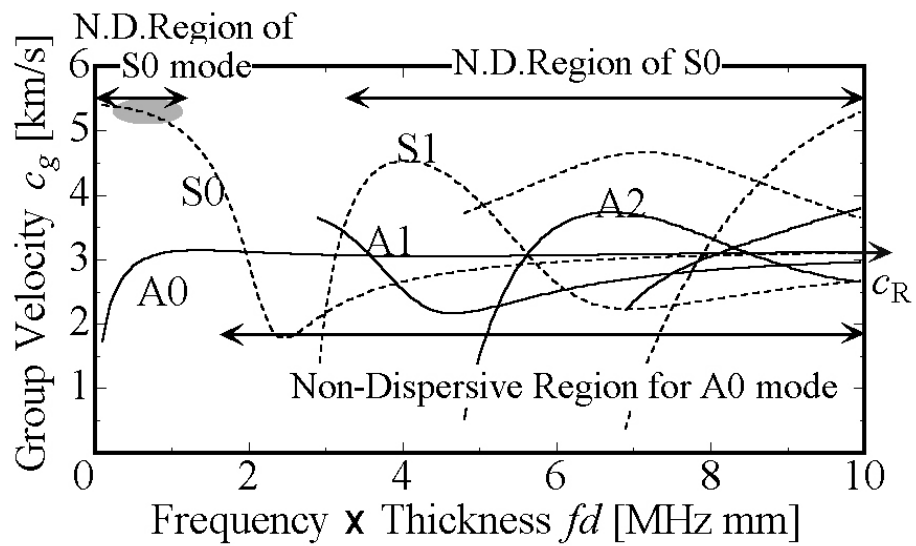
(b) Group velocity

Figure 2 Takahiro Hayashi
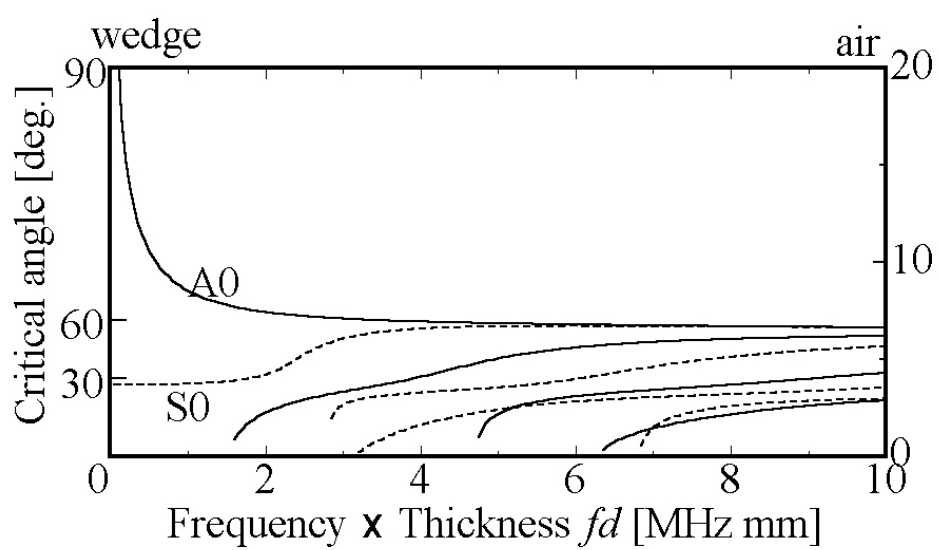
Figure 3   Takahiro Hayashi
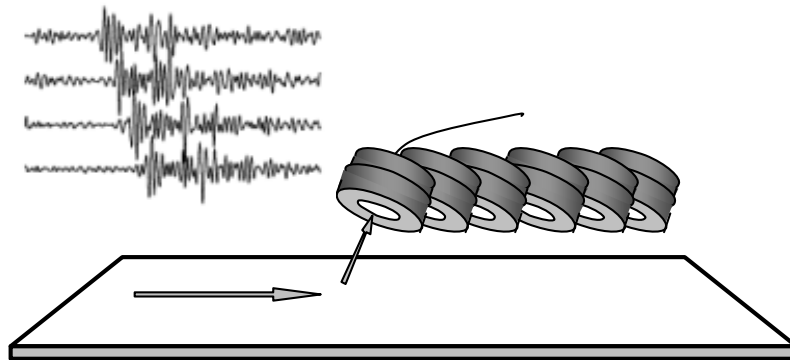
(a) Wave detection at regularly spaced points
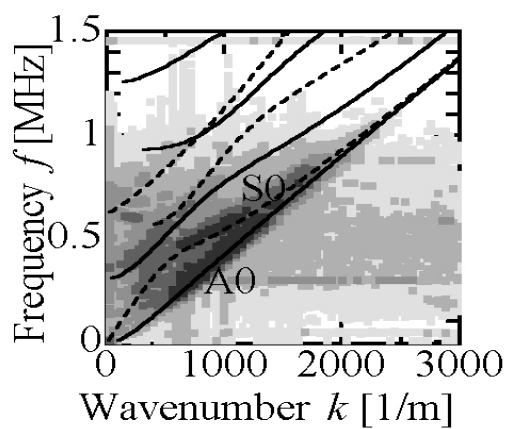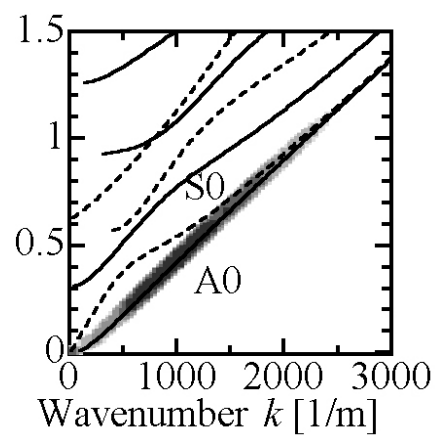
(b) *k-f* distribution image   (c) *k-f* image after filtering
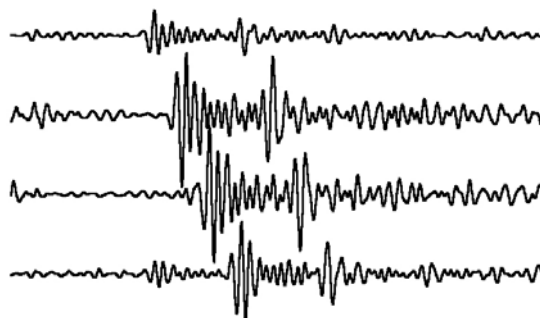
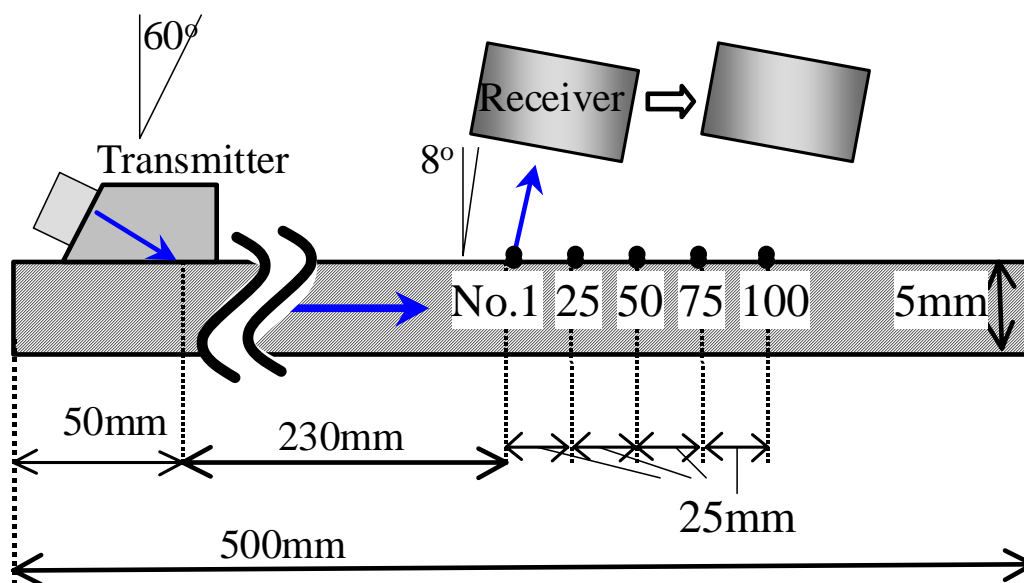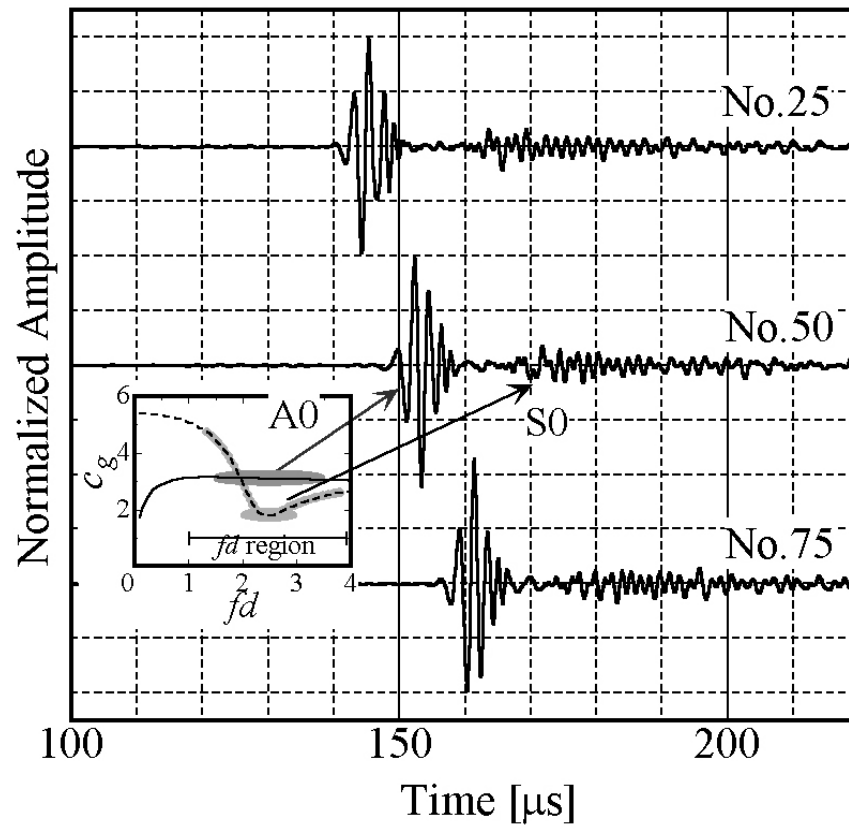(d) Filtered waveforms

Figure 4
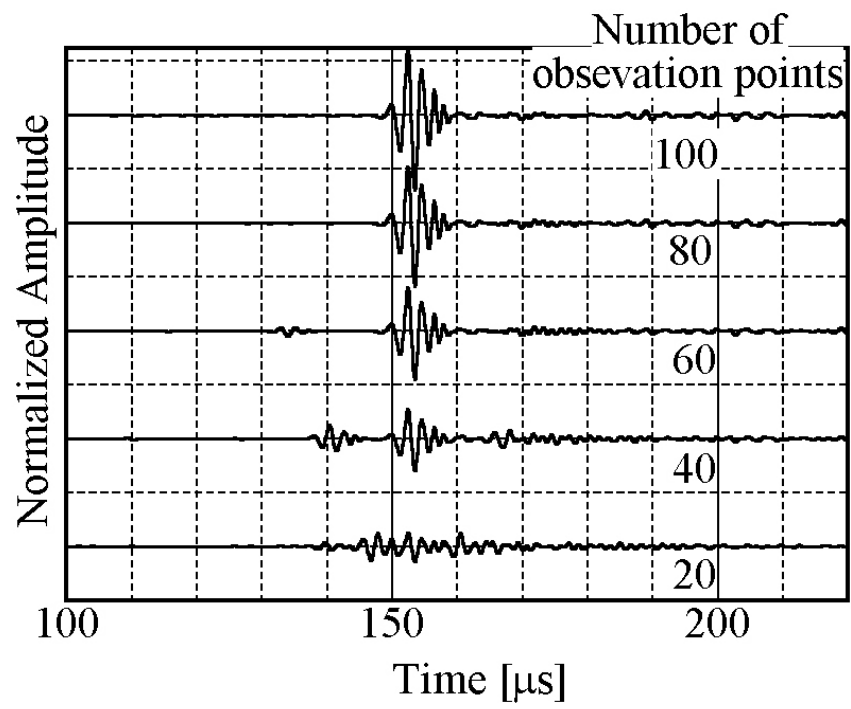
Takahiro Hayashi

Figure 5   Takahiro Hayashi

Figure 6

Takahiro Hayashi
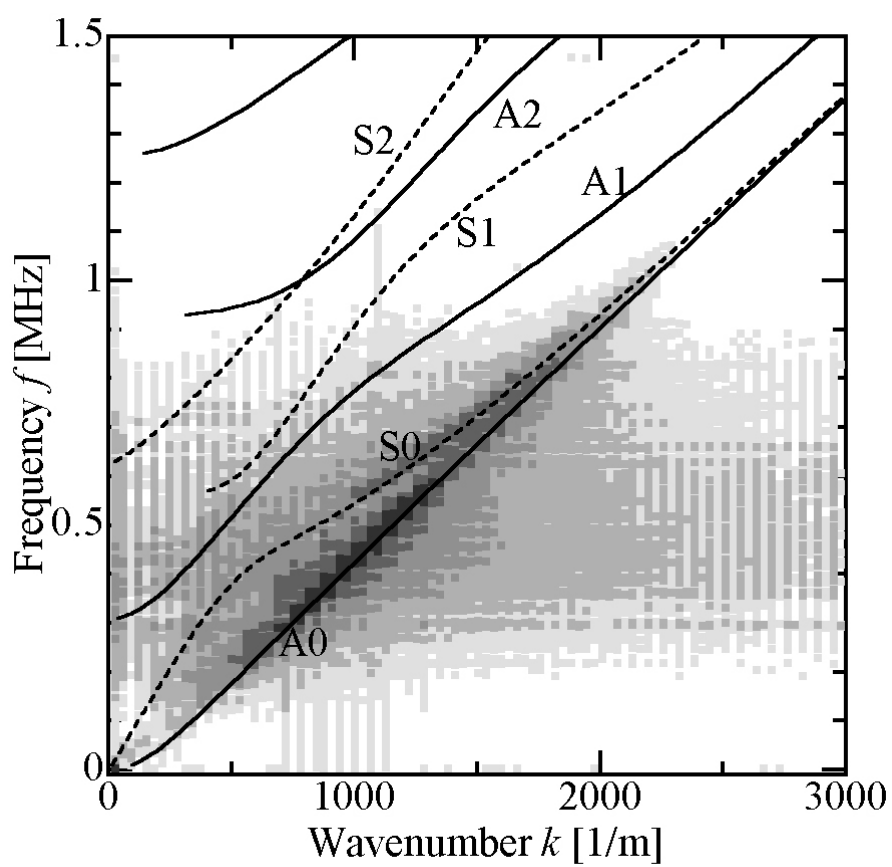
Figure 7

Takahiro Hayashi
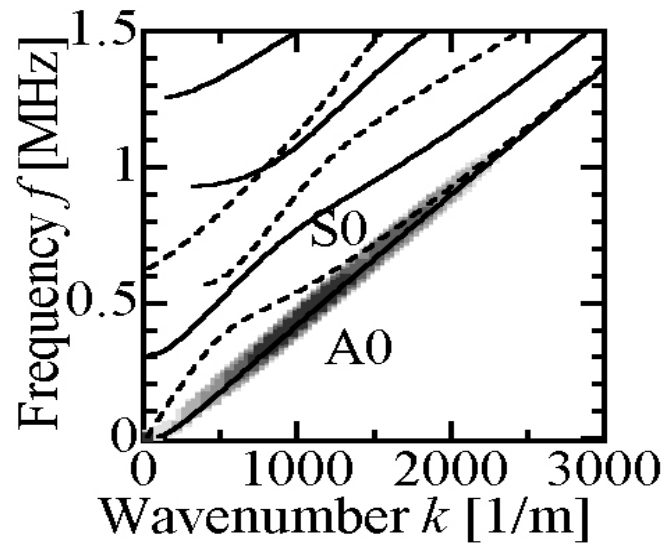
(a) A0 mode extraction
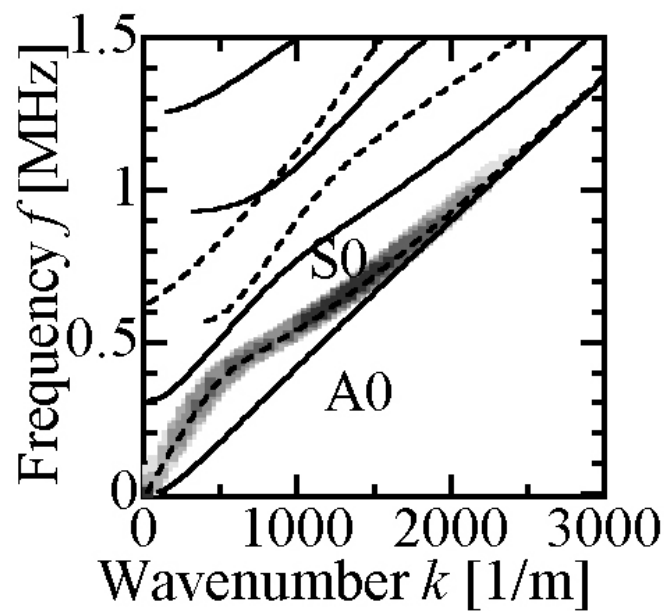
(b) S0 mode extraction

Figure 8

Takahiro Hayashi
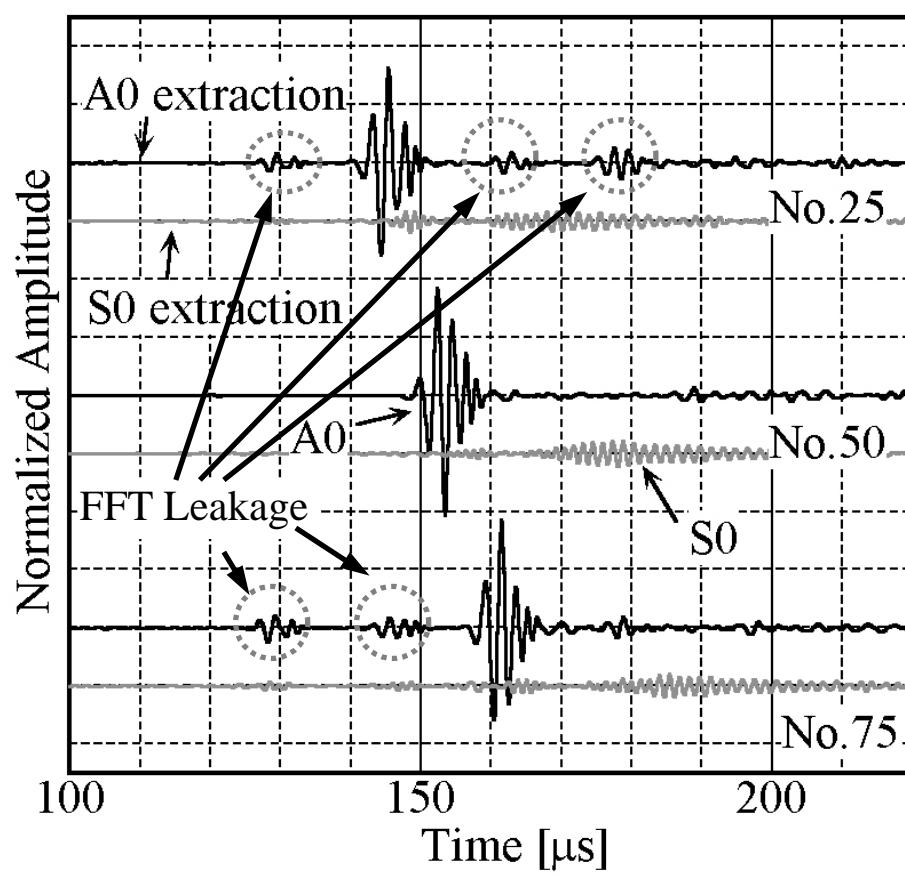
Figure 9   Takahiro Hayashi
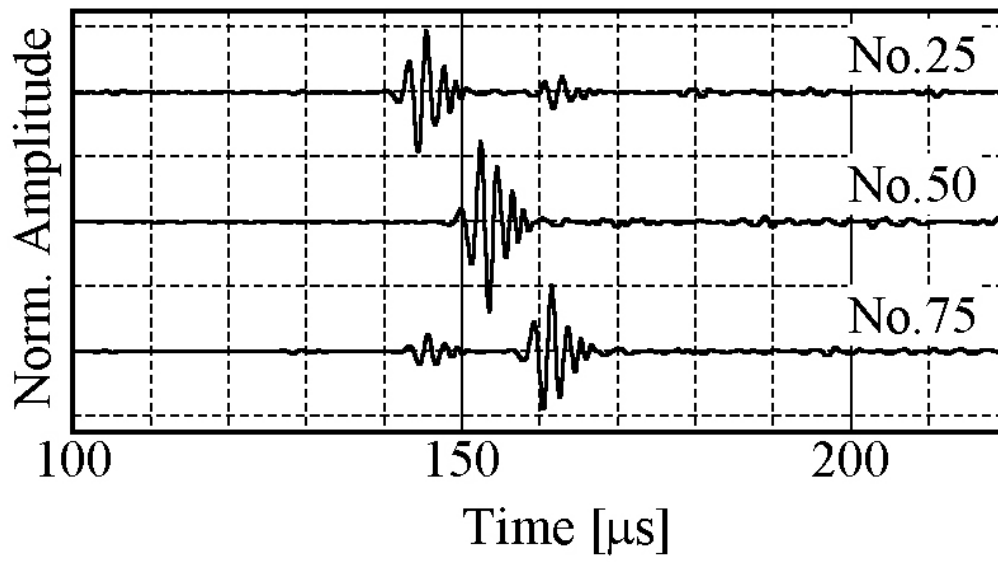
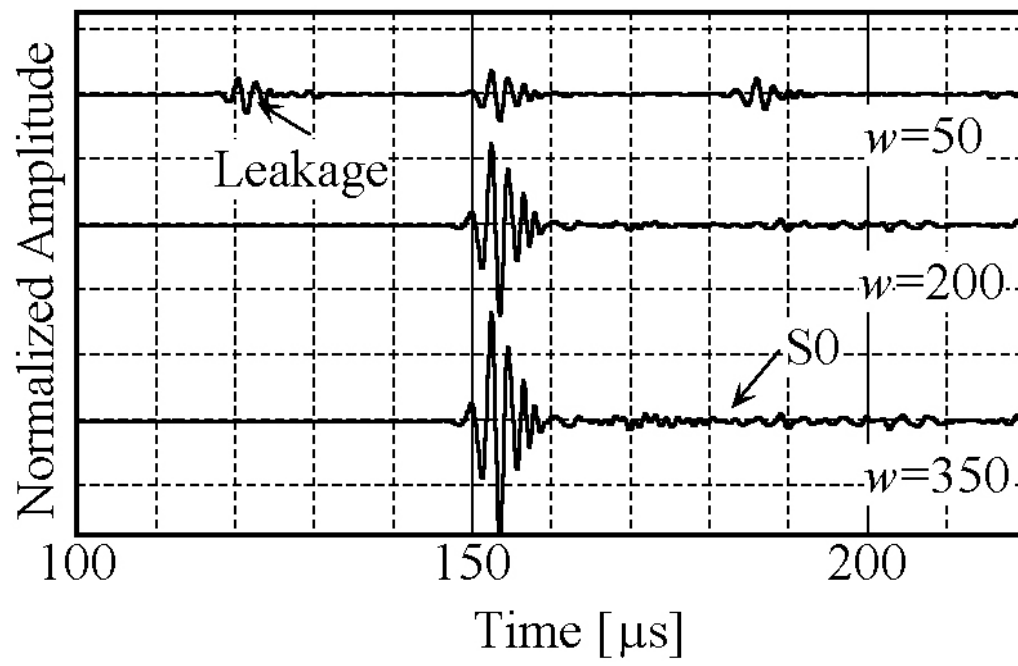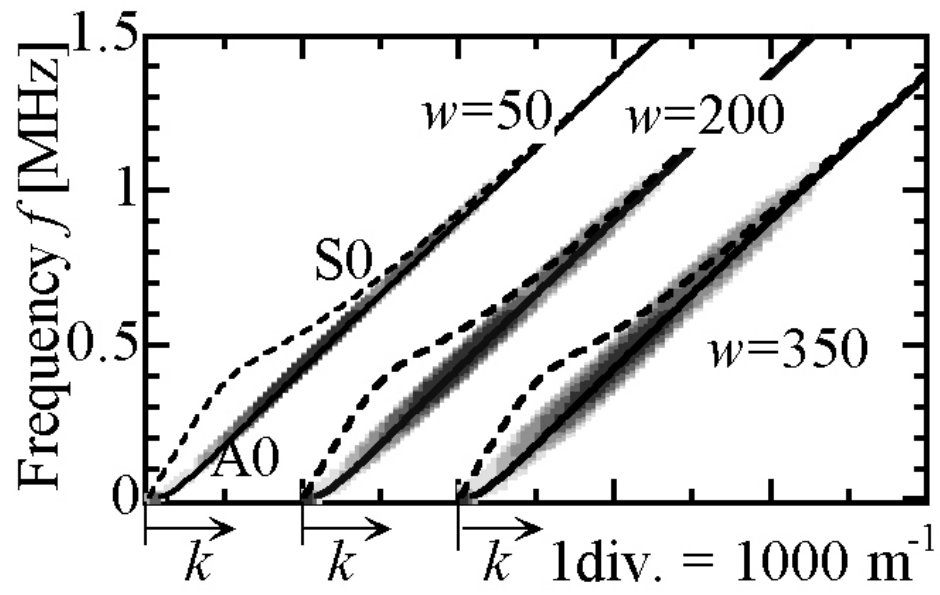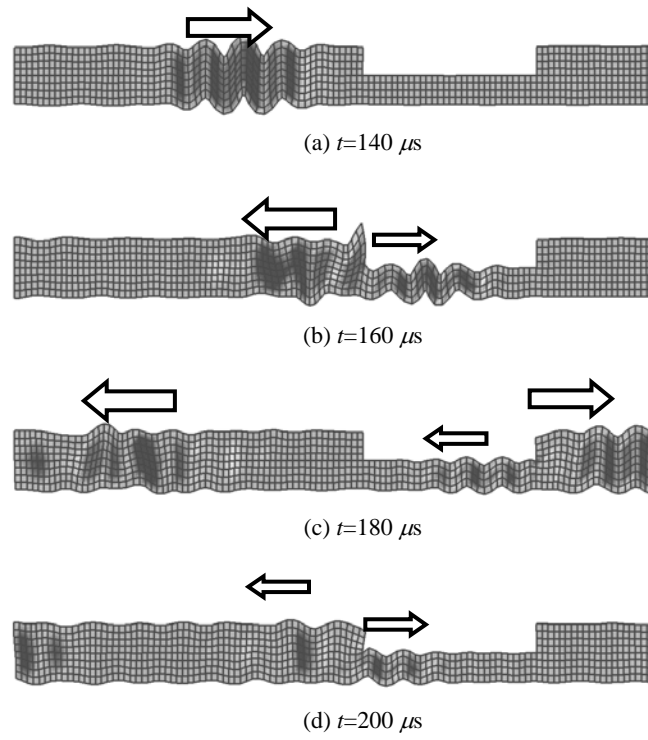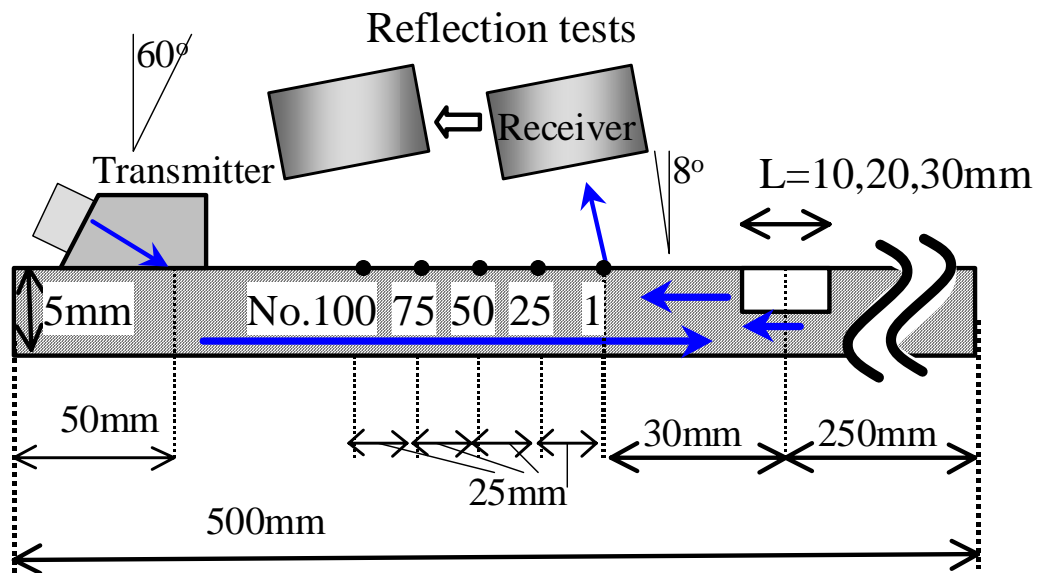Figure 10   Takahiro Hayashi

Figure 11 Takahiro Hayashi

Figure 12

Takahiro Hayashi

Figure 12

Figure 13   Takahiro Hayashi

(a) t=140 μs

(b) t=160 μs

(c) t=180 μs

(d) t=200 μs

Figure 14 Takahiro Hayashi

Figure 15   Takahiro Hayashi
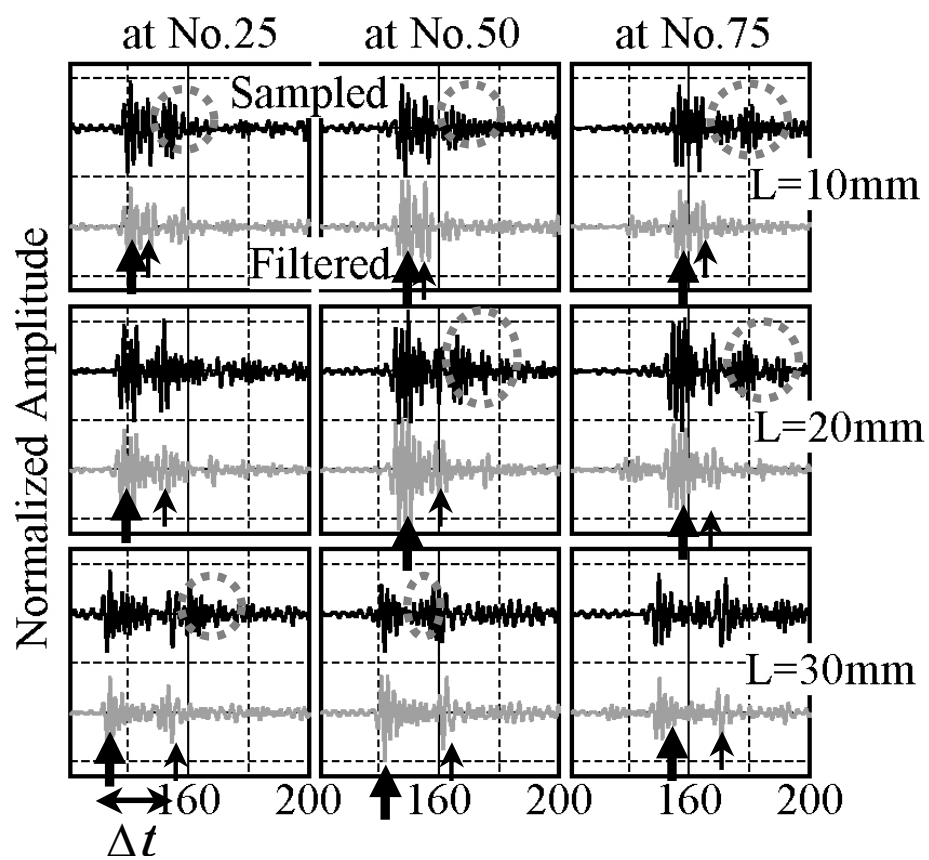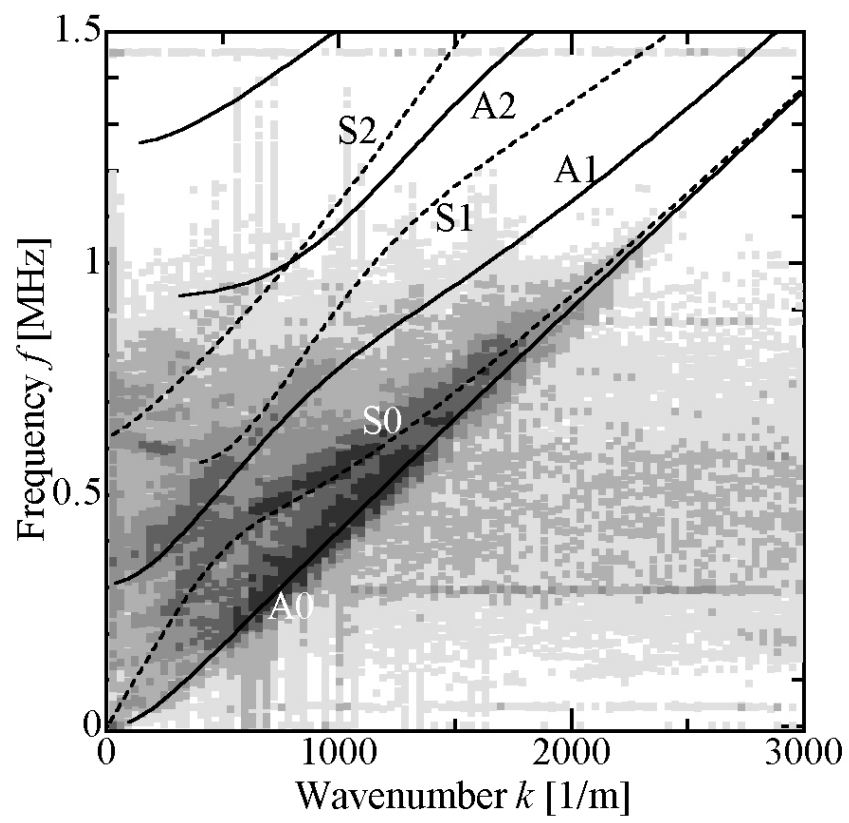
Figure 16   Takahiro Hayashi

Figure 17
Takahiro Hayashi